Available online at www.sciencedirect.com
SCIENCE DIRECT®
ELSEVIER
International Journal of Mass Spectrometry 228 (2003) 1055–1065
International Journal of Mass Spectrometry
www.elsevier.com/locate/ijms

Implanting atomic ions into surface adsorbed fullerenes: the single collision formation and emission of $Cs@C_{60}^+$ and $Cs@C_{70}^+$

A. Kaplan, Y. Manor, A. Bekkerman, B. Tsipinyuk, E. Kolodney*

Department of Chemistry, Technion—Israel Institute of Technology, Haifa 3200, Israel

Received 13 December 2002; accepted 28 April 2003

Abstract

We describe the formation and emission of endohedral fullerenes, $Cs@C_{60}^+$ and $Cs@C_{70}^+$, following a single collision of Cs^+ ion with a sub-monolayer of C_{60} on gold and silicon surfaces and with a sub-monolayer of C_{70} on gold. A continuous low energy (E_0 = 35–220 eV) Cs^+ ion beam hit the C_{60} covered surface and the collisional formation and ejection of the endohedral $Cs@C_{60}^+$ complex, within a single Cs^+/C_{60} collision, was observed and characterized. The steady state C_{60} coverage is shown to be in the sub-monolayer range. The instantaneous rise of the $Cs@C_{60}^+$ signal (by a factor of 10^3) with the Cs^+ beam onset clearly demonstrate the single collision nature of the combined "atom penetration/endo-complex ejection" event. The fullerene molecule is actually being picked up off the surface by the penetrating Cs^+ ion. The evidence for the trapping of the Cs^+ ion *inside* the fullerene cage is given both by the appearance of the $Cs@C_{60-2n}^+$ (n = 1–5) sequence and its termination at $Cs@C_{50}^+$. Similar experiments were carried out with nearly pure (98%) C_{70} sub-monolayer on gold. Both the $Cs@C_{70-2n}^+$ and C_{70-2n}^+ ($n = 0, 1, 2, \ldots$) fragmentation sequences were observed. $Cs@C_{60}^+$ and C_{60}^+ signals appeared strongly enhanced in these sequences. We believe that the experimental results presented here provide a first example of a single collision pick-up scattering (Eley–Rideal type) involving the formation and ejection of an endo-complex.

Keywords: Endohedral fullerenes; Surface scattering; Eley–Rideal reactions; Ion implantation

1. Introduction

Unique species and interesting chemical binding configurations are often identified among the scattered particles following energetic projectile-target encounters. The projectile impact energy E_0 provides the necessary activation energy for the reactive scattering event. Various examples can be found in studies of sputtering from surfaces using energetic atomic ion beams and in pick up reactive scattering with molecular ions. In secondary ion mass spectrometry (SIMS) experiments on organic layers with Cs^+ as the primary beam, adducts in the form of CsM^+ are frequently observed, where M is an organic or inorganic residue [1]. Similar Cs^+ bombardment experiments on a graphite target yield species of the form CsC_n^- (n = 4, 6, 8, etc.) [2]. In all cases reported the outgoing sputtering or pick-up product is an exo-complex, where the two collision partners are attached side by side. In order to get an endo-complex where the incoming atomic ion is encapsulated inside a very large molecule or cluster one needs to be able to implant the primary

* Corresponding author. Tel.: +972-4-8293749; fax: +972-4-8295703.
E-mail address: eliko@tx.technion.ac.il (E. Kolodney).

1387-3806/$ – see front matter © 2003 Elsevier B.V. All rights reserved.
doi:10.1016/S1387-3806(03)00269-0

ion into the target specie and the target specie should be able to anneal itself, namely regaining the original structure or rearrange itself around the implanted ion in some stable configuration. Here we describe a collision experiment resulting in the formation and ejection of an endo-complex, within a single collision. We will review some recent observations [3] and extend it to new surface/collider systems. Low energy (E_0 = 30–220 eV) Cs^+ ions hit and penetrate C_{60} molecules adsorbed on gold and silicon surfaces. Care was taken to assure sub-monolayer steady state coverage of the C_{60} molecules. The penetrating Cs^+ atom is therefore backscattering inside the open fullerene cage after hitting the inner side of the carbon network, which is in contact with the substrate itself. The time scale for the backscattered Cs^+ atom to escape through the window which is temporarily opened in the C_{60} cage (breaking of carbon–carbon bonds upon the penetration impact) is probably sub-picosecond. The fact that we observe the formation of intact (but highly vibrationally excited) endohedral fullerene is a striking evidence for the extremely efficient self-healing abilities of the fullerene carbon cage. The trapped atom, after intra-cage back and forth scattering accompanied by vibrational heating of the cage, still has enough backward momentum in order to enable the ejection of the endo-complex from the surface.

Besides of being an example for a unique pick-up scattering resulting in the combined formation/ejection of an endo-complex, there is a lot of interest specifically in the formation mechanisms and synthesis of endohedral fullerenes [4,5]. Ion implantation into substrate supported C_{60} was shown to have a promising potential as a general M@C_{60} (M as an alkali atom) high yield production method. Campbell and co-workers were the first to demonstrate this experimentally [6,7]. They have bombarded thin C_{60} films deposited on a Si substrate by M^+ alkali ion beams (M = Li, Na, K, Rb). By post-analyzing (ex situ) the films using laser desorption mass spectrometry they have found that the materials so-produced contains M@C_{60}. A yield of up to 50% was reported for Li@C_{60} and 2–5% for the larger alkali ions [7]. Bombardment with Cs^+ ions was not attempted in these experiments. Similar ion beam implantation method with deposited C_{60} was reported also for He^+ and Ne^+ ions but with an efficiency of only up to 0.05% [8]. While the beam-surface approach was introduced only as a high yield synthetic method (for alkali ions), without any in-situ characterization, former gas phase experiments provided deeper insight into the dynamics and energetics of the endohedral formation process. Schwarz and co-workers performed the first experiments in this field by passing high-energy C_{60}^+ ions through helium [9] and other rare gases [10]. Anderson and co-workers have used atomic ion beams at kinetic energies of E_0 = 0–150 eV for implanting Rg^+ rare gas ions and some M^+ alkali ions (Li^+, Na^+, K^+) into neutral fullerene molecules (C_{60}/C_{70} vapors) [11–13]. The main information source for the penetration dynamics in the gas phase experiments is the kinetically shifted E_0-dependent yield curves for the M@C_{60-2n}^+ and Rg@C_{60-2n}^+ ions ($n = 0, 1, 2, \ldots$). These curves are directly related to the vibrational excitation of the endohedral complex during its collisional formation. The experiments presented here are in a way a marriage of both approaches: The fullerene molecule is directly supported on a solid substrate and the fragmentation dynamics of the vibrationally hot outgoing endohedral complex is probed on-line as a function of impact energy. The ability to change the supporting substrate thus controlling (indirectly) the energy loss of the impinging ion to the surface (and subsequently the vibrational heating of the endohedral fullerene) is an important additional degree of freedom. The energy transfer to the substrate is obviously mediated by the carbon cage since the penetrating ion is hitting the inner side of the fullerene molecule (via a single or multiple intra-cage scattering) which is in direct contact with substrate atoms.

Finally, the experiments presented here are aimed at providing better understanding of the collisional formation of endohedral fullerenes at surfaces. This aspect can be broadened to ion implantation into nano-structures in general. It could be expected that interest in controlled, low energy (<500 eV) ion implantation into carbon-based inorganic and organic nano-structures on surfaces will grow sharply together

with the increase in number of applications in nano-electronics. Two specific examples are carbon nanotubes (where the amount of implanted core ions inside the nanotube controls electrical properties) [4] or organic nano-structures based on self-assembled monolayers where implanted ions could control electron transfer properties.

2. Experimental

The experimental set-up is presented in Fig. 1. An effusive C_{60} beam emerging from a C_{60} oven, served for depositing C_{60} molecules on the gold and silicon surfaces. The beam axis was at 45° to the surface normal. A Cs^+ ion gun, also situated at 45° to the surface normal (and at 90° to the C_{60} beam axis) delivered beam currents of 1–10 nA at energies of up to 250 eV with an energy width of 0.5 eV or smaller (FWHM). During normal operation both the C_{60} oven and the Cs^+ ion gun are working simultaneously such that a steady state C_{60} coverage and stable $Cs@C_{60}^+$ and $Cs@C_{70}^+$ currents are achieved. The scattered species and their (on-flight) dissociation products are collected by ion-extraction and ion-transfer optics into quadrupole mass spectrometer (QMS; Extrel MEXM-4000) whose axis is along the surface normal. Pure C_{60} (MER, 99.8% purity) and C_{70} (MER, 98% purity; 0.3% C_{60} impurity) powders were used. The experiments were conducted inside an ultrahigh-vacuum chamber (base pressure: 5×10^{-10} Torr). The C_{60} source was thermally isolated from its surroundings by three concentric Ta radiation shields. The final C_{60} beam spot at the surface was about 10 mm in diameter (actually an ellipsoidal projection). The Cs^+ ion beam spot on the surface was about 2 mm in diameter thus assuring nearly homogeneous C_{60} density within the Cs^+ impact zone. The effusive neutral Cs beam component was blocked by tilting the Cs^+ ion beam 2–3° off-axis. Please note that the E_0-dependent yield curves presented here are not measured under field free conditions and therefore are not easily amenable to detailed kinetic analysis. The target potential was +10 V and the QMS

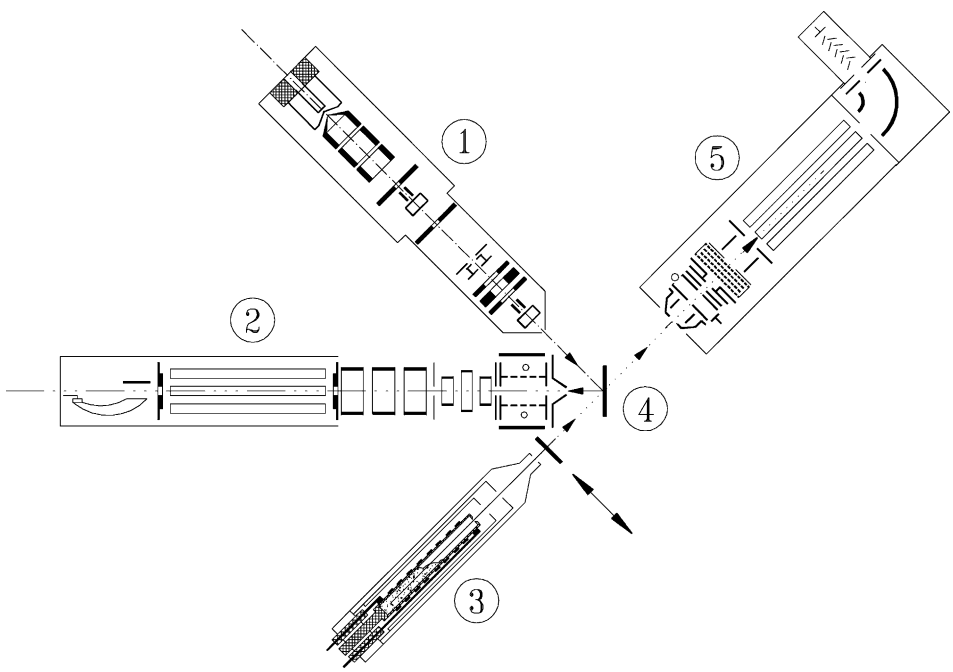

Fig. 1. The experimental set-up: (1) Cs^+ ion gun; (2) quadrupole mass analyzer with ion transfer and extraction optics; (3) fullerene oven for nearly collimated effusive beam; (4) rotatable surface; (5) quadrupole mass spectrometer on-line with the effusive fullerene beam.

extraction electrode potential was −20 V for optimal collection of all secondary positive ions. Field free measurements aimed at testing kinetic models will be carried out at a later stage.

Suitable substrates for achieving sub-monolayer coverage of C_{60} and C_{70} are those where the interaction between the fullerene molecule and the substrate atoms is stronger than the C_{60}–C_{60} or C_{70}–C_{70} interaction which to a good approximation is given by the heat of sublimation of the solid (1.4 eV/molecule for C_{60} [14]). If this is not the case the fullerene molecule will tend to form 3D islands even at low surface concentrations. The heat of adsorption for fullerenes on Au and Si is 2.0–2.5 eV/molecule [4,15,16]. Therefore, a completion of sub-monolayer or full monolayer growth can be expected before islanding. For a Si surface, the fullerene-surface bond energy should be somewhat higher than for a Au surface due to high density of dangling bonds. It was reported that most of the C_{60} molecules adsorbed on Si(1 0 0)–(2 × 1) are located over the silicon surface dimer row (between four dimers), forming a partially ordered overlayer [17]. For the experiments reported here we have used hyperpure epitaxial Si(1 0 0) wafer and polycrystalline gold surface. Both surfaces were sputtered/annealed with an Ar atom gun at temperature of about 950 K before every run. For the gold surface, an optical goniometry check (with He–Ne laser through a set of slits) combined with surface microscopy showed that the annealed surface is composed off large (∼1 mm^2) crystallites whose planes are all parallel to each other and to the macroscopic surface plane to within ±0.5°. During the initial C_{60} deposition and throughout all experiments reported here the surface was kept at room temperature.

3. Results and discussion

3.1. Collisions of Cs^+ ions with the C_{60}/Au target

The experiment is being carried out under steady state conditions between C_{60} deposition (layer growth) and Cs^+ ion beam etching (layer removal via $Cs@C_{60}^+$ ejection and C_{60}^+ sputtering). Both C_{60} deposition rate and Cs^+ beam current were kept low (in the range of 1 monolayer per 200–400 s) in order to maintain a balance between layer growth and etching. All experimental evidence point out that the resulting deposition/etching steady state was at sub-monolayer coverage [3]. The main evidence is provided by the Langmuir-type first-order growth kinetics of the $Cs@C_{60}^+$ and C_{60}^+ ion signals observed as a function of the C_{60} deposition time, under constant Cs^+ ion flux. A time constant of 120 s and a saturation value near 200 s were measured. Under these conditions we have found that the formation of the endohedral fullerene is practically instantaneous with the opening time of the Cs^+ ion beam. As shown in Fig. 2, when C_{60} is being deposited on the surface for 5–10 min and then the Cs^+ ion beam is suddenly turned on, the $Cs@C_{60}^+$ signal is instantly increasing by a factor of 10^3. There is no need for any preconditioning of the surface such as slow build up of $Cs@C_{60}$ or pure Cs densities at the surface. Any process like this will result in a slow signal increase with a few hundreds of seconds rise time (due to the low Cs^+ ion flux). Actually, the signal decays from its peak value by about 30% over 300 s of Cs^+ bombardment. This slow layer depletion

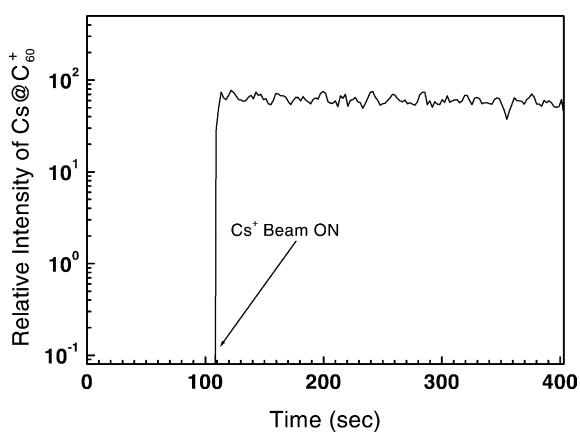

Fig. 2. Instantaneous rise of the $Cs@C_{60}^+$ signal (by a factor of 10^3) with the Cs^+ beam opening. The surface was pre-exposed to the C_{60} beam for 5–10 min. The slow decay of the signal from its peak value (by about 30% over 300 s) is due to depletion of the C_{60} coverage by C_{60}^+ and $Cs@C_{60}^+$ ejection and is consistent with the measured sputtering rate.

is in good agreement with the measured sputtering rate. The experiment presented in Fig. 2 can be considered as a clear evidence that both the formation and the ejection of the endohedral fullerene constitute a combined (nearly simultaneous) event, which occurs within a single Cs^+ collision. Please note that in this paper we do not address the issue of the extent of impulsiveness of the ejection process. By saying "single collision" we simply mean that the same Cs^+ ion penetrating the C_{60} cage is responsible for lifting the just-formed $Cs@C_{60}$ off the surface. However, we argue that the just-formed $Cs@C_{60}$, while still on the surface, cannot suffer more than a few intra-cage Cs^+ chattering events before lift-off. Namely, its expected residence time on the surface will be a few picoseconds or less (probably even below one picosecond). Longer residence time will inevitably lead to efficient thermal accommodation to the surface resulting in substantial fraction of the endohedral complex left on the surface. This will be in clear disagreement with the experimental observation reported earlier in this paper which showed no accumulation of $Cs@C_{60}$ on the surface. Furthermore, a preliminary temperature programmed desorption (TPD) measurement after about 90 min of simultaneous Cs^+ bombardment and C_{60} deposition failed to detect any $Cs@C_{60}$ desorption peak over the 320–970 K surface temperature range. Additional experimental evidence for the very short residence time of $Cs@C_{60}$ on the surface (one or few Cs^+ intra-cage scattering events before lift-off) is provided by recent measurements we have carried out of the kinetic energy distributions of the outgoing $Cs@C_{60}^+$ [18]. The measured distributions were found to be non-thermal, peaking around 1.2 eV with substantial fraction of the outgoing endohedrals having kinetic energy above 2 eV. These observations practically exclude the possibility of thermal desorption following vibrational coupling to the surface (even for a few thousands °C temporarily induced local hot spot at the surface).

During bombardment of the C_{60} overlayer with the Cs^+ ion beam (E_0 = 35–220 eV), both endohedral $Cs@C_{60}^+$ and C_{60}^+ ions were ejected off the surface. The apparent (extrapolated) appearance energy of $Cs@C_{60}^+$ is around 35–40 eV while that of C_{60}^+ is

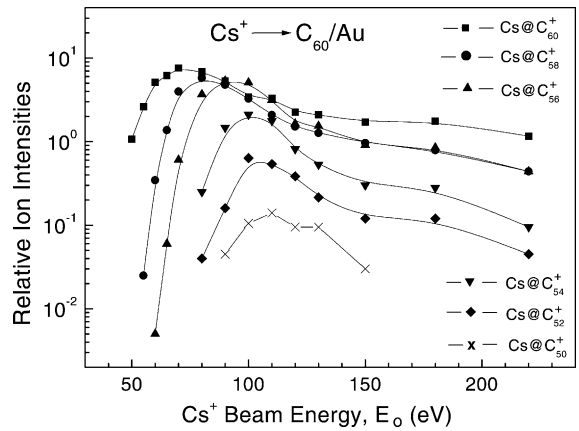

Fig. 3. Relative intensities of the parent endohedral complex ion $Cs@C_{60}^+$ and its daughter ions $Cs@C_{60-2n}^+$ (n = 1–5) as a function of the Cs^+ ion energy over the energy range E_0 = 50–220 eV. The surface is C_{60}/Au. All ion intensities are normalized to the Cs^+ beam current.

50 eV. The onset for the fragmentation of the vibrationally hot $Cs@C_{60}^+$ and C_{60}^+ is at 55 eV. The evolution of the fragmentation pattern of both endohedral and empty parent specie was measured over the E_0 range of 50–220 eV. Fig. 3 shows the E_0-dependent $Cs@C_{60-2n}^+$ (n = 0–5) ion intensities while Fig. 4 shows the E_0-dependent C_{60-2n}^+ (n = 0–8) ion intensities. The sequential emission of up to five C_2 units while retaining the Cs^+ ion attached to the fullerene, rather than immediate emission of the Cs^+ by the vibrationally hot $Cs@C_{60}^+$, provides a clear evidence for the endohedral nature of the complex. Several important observations emerge from Figs. 3 and 4. First, the $Cs@C_{60}^+$ and C_{60}^+ yields have strong maximum around 70–100 eV impact energy. Second, all the breakdown curves are kinetically shifted with respect to each other as expected from sequential delayed fragmentation of energy-rich endohedral and empty fullerenes in gas phase experiments [12]. And third, the parent $Cs@C_{60}^+$ seems to be much hotter than the parent C_{60}^+. The last point provides further evidence for the single collision nature of the penetration/ejection event, as opposed to the alternative case of sputtering of pre-produced endohedral fullerenes by the Cs^+ ion beam. If the $Cs@C_{60}$ was already thermally accommodated to the surface, then its internal vibrational temperature

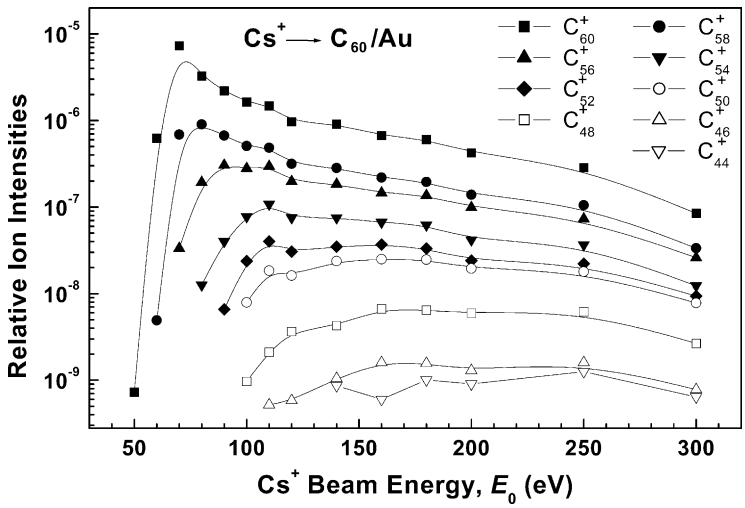

Fig. 4. Relative intensities of the sputtered C_{60}^+ ion and its daughter ions $Cs@C_{60-2n}^+$ ($n = 1$–8) as a function of the Cs^+ ion energy over the energy range $E_0 = 50$–300 eV. The surface is C_{60}/Au. All ion intensities are normalized to the Cs^+ beam current.

should not be higher than that of the sputtered C_{60}^+. The important conclusion is that the fragmentation pattern is a fingerprint that carry direct information on the collisional formation dynamics of the $Cs@C_{60}^+$. This involves the initial deformation, penetration (bonds breaking), cage annealing (bonds forming) and intra-cage chattering of the trapped Cs^+ ion. In Fig. 5 we present the impact energy dependent integrated yields of $Cs@C_{60}^+$ and C_{60}^+ scattered off the surface. We are assuming that only $Cs@C_{60}$ and C_{60} (neutral or ionized) are ejected off the surface and fragmentation occurs on-flight. The $Cs@C_{60}^+$ yield curve peaks at $E_0 = 80 \pm 5$ eV. The mechanisms leading to the ionization are not clear yet. Probably there are meaningful contributions from both surface charge exchange and delayed thermionic emission. It is well known that isolated highly vibrationally excited fullerenes emits electrons on a time scale of hundreds of microseconds [19,20]. Kinetic energy distributions of outgoing $Cs@C_{60}^+$ and C_{60}^+ measured with a potential gradient between the surface and the extraction electrode [18] appear to have a component of "negative apparent energies" (after subtracting the acceleration voltage). This is an indication for ion formation away from the surface. Namely, the ions born along the flight path due to delayed electron emission do not experience the full acceleration voltage (Fig. 5).

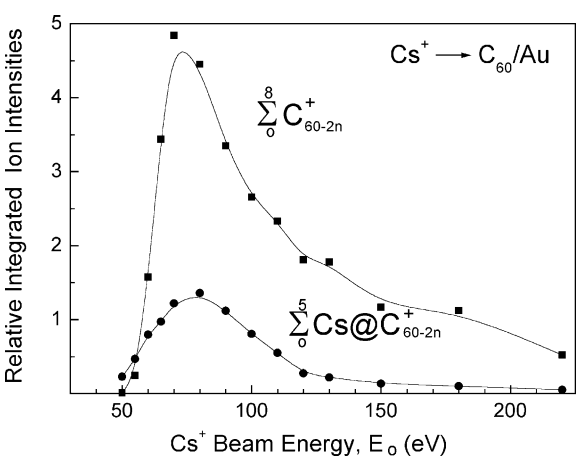

Fig. 5. Relative $Cs@C_{60}^+$ and C_{60}^+ yields (E_0 dependent) calculated by summing over all the measured breakdown curves as presented in Figs. 3 and 4.

3.2. Collisions of Cs^+ ions with C_{60}/Si target

The nature of the C_{60}/Si interaction was already discussed in Section 2. The (scattered) positive ion mass spectra following Cs^+ ion bombardment was measured over the impact energy range $E_0 =$ 50–220 eV. The threshold value for $Cs@C_{60}^+$ formation

is slightly higher than for the C_{60}/Au system and is around $E_0 = 45$ eV. Typical spectra for several E_0 values are shown in Fig. 6. At $E_0 = 55$ eV the mass spectrum is dominated by $Cs@C_{60}^+$ and C_{60}^+ signals. Both outgoing molecules are too cold to emit C_2 units during the experimental time window. A small mass peak at around 986 amu is probably due to the exo-endohedral fullerene Cs ($Cs@C_{60}^+$) formed when a leaving $Cs@C_{60}^+$ picks up a Cs atom on its way out. The strong relative decrease in the intensity of this peak at higher impact energies is in agreement with this assignment since it is expected that hotter endohedrals will efficiently emit the exo-atom before reaching the detector. The mass spectra at $E_0 = 90$ and 120 eV clearly show that the $Cs@C_{60}^+$ ions are hotter than the sputtered C_{60}^+ ions. This conclusion is based on the relative intensities of the $Cs@C_{60-2n}^+$ and C_{60-2n}^+ mass peaks within each sequence since the fragmentation time windows for both ions are similar and the Arrhenius parameters for C_2 emission are assumed to be roughly the same for $Cs@C_{60}^+$ and C_{60}^+. The last assumption is probably reasonable for the parent species and their daughter ions down to $Cs@C_{54}^+$ (when the cage is not yet tightly wrapped around the central Cs atom) but may be questionable when approaching the sequence end-point at $Cs@C_{50}^+$. Fig. 7 shows the fragmentation pattern at $E_0 = 110$ eV with an expanded section for the 700–880 amu mass range. The $Cs@C_{60-2n}^+$ end point at $n = 5$ is demonstrated by the absence of the $Cs@C_{48}^+$ signal at mass 709 amu (indicated by an arrow). This minimal possible size for the endohedral fullerene formed by the "shrink wrap" mechanism probably reflects the size of the smallest fullerene that can still contain the central atom without falling apart [21,22]. Similar behavior was observed for $Cs@C_{60}^+$ on gold. The E_0-dependent yields of the $Cs@C_{60-2n}^+$ daughter ions are shown in Fig. 8. Based on the relatively high intensity of the $Cs@C_{56}^+$ signal it seems that the $Cs@C_{60}^+$ formed on the Si surface is somewhat hotter than the one formed on the Au surface. This tendency is in line with the higher Debye temperature for the Si surface as compared with Au [23] (which means that the Si surface is less responsive than the Au surface). However,

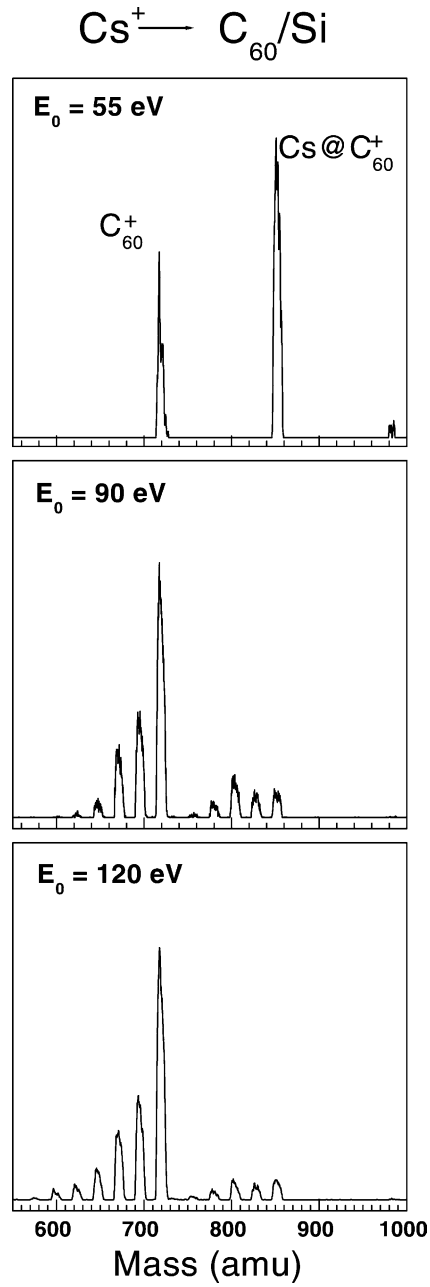

Fig. 6. Positive ion mass spectra following Cs^+ ion impact ($E_0 = 50$–220 eV) on a C_{60}/Si surface. Note the gradual evolution of the fragmentation pattern for both $Cs@C_{60}^+$ and C_{60}^+ ions.

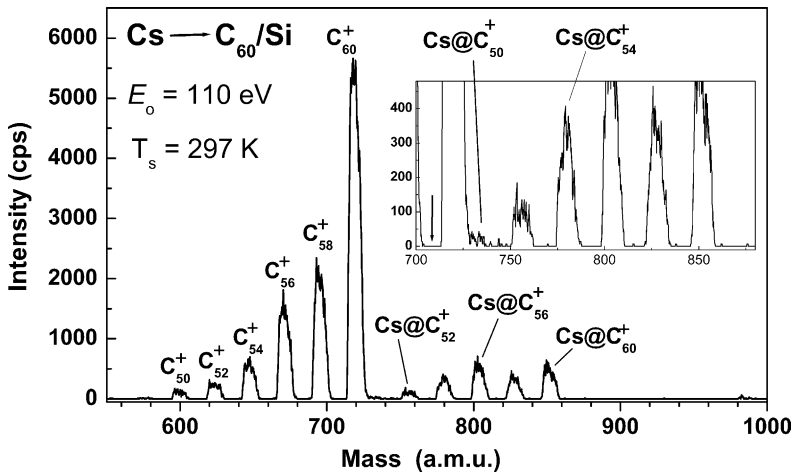

Fig. 7. Fragmentation of $Cs@C_{60}^+$ and C_{60}^+ ions formed by Cs^+ ion impact ($E_0 = 120$ eV) on a C_{60}/Si surface. The inset shows the termination of the C_2 emission sequence at $Cs@C_{50}^+$. The arrow points at the location of the (missing) $Cs@C_{48}^+$ daughter ion at 709 amu.

in order to get a better idea about the energy loss to the surface and the final vibrational excitation of the outgoing $Cs@C_{60}^+$ one needs to know also the effective masses for the two different collision events, in the C_{60}/Au and C_{60}/Si systems. Comparative measurements of kinetic energy distributions for the outgoing $Cs@C_{60}^+$ on these systems will provide a deeper insight into this problem.

3.3. Implanting Cs^+ ion into C_{70} molecules deposited on a gold surface

The same measurements reported earlier in this paper for C_{60} deposited on a gold surface were carried out also with C_{70}, resulting in the formation of $Cs@C_{70}^+$ and its daughter ions. In carrying out these experiments we were mainly motivated by the

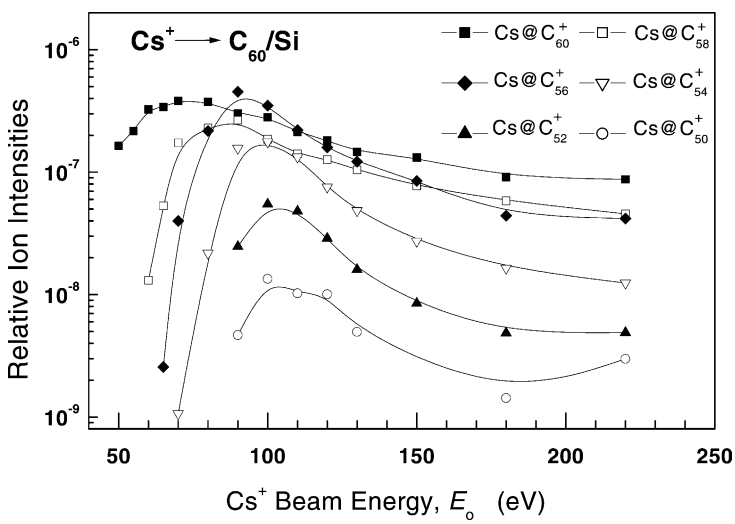

Fig. 8. Relative intensities of the parent endohedral complex ion $Cs@C_{60}^+$ and its daughter ions $Cs@C_{60-2n}^+$ ($n = 1$–5) for a C_{60}/Si surface as a function of the Cs^+ ion energy over the energy range $E_0 = 50$–220 eV. All ion intensities are normalized to the Cs^+ beam current.

different bonds structure of C_{70} and C_{60} and the assumption that the efficient penetration and cage annealing observed for C_{60} is directly related with the specific hexagons/pentagons arrangement of a given fullerene molecule and that different behavior (e.g., impact energy dependence) may be observed with C_{70}. While C_{60} has one unique carbon site and two distinct bond lengths C_{70} has five inequivalent sites and eight distinct bond lengths. Here we give only a brief preliminary report describing our observations.

In order to deposit nearly pure C_{70} sub-monolayer on the gold substrate we have started from a 98% C_{70} powder, which was loaded into the effusive fullerene beam oven. A new ceramic cartridge was used to this purpose and the Ta radiation shields were thoroughly cleaned from any traces of C_{60}. The issue of the final composition of the effusive beam with respect to the initial C_{70}:C_{60} ratio in the solid mixture is not simple and depends strongly on the nature of the starting material (the C_{70} powder): amorphous or polycrystalline, percentage of fully intercalated C_{70}–C_{60} crystallites, etc. [24,25]. Partial pressures of C_{60} and C_{70} were measured before as a function of temperature for solid C_{70}:C_{60} samples with different compositions ranging from pure C_{60} to pure C_{70} (but only up to 71 mol% C_{70}-rich mixture) [25]. It was argued that the C_{70}:C_{60} binary system forms a solid solution where the two components are partially miscible up to 30 mol%. A binary phase diagram was derived based on the varying vapor pressures of C_{60} and C_{70} in the sublimed samples [25]. In this case our nearly pure C_{70} powder can be considered almost an ideally dilute solution with no solute–solute (C_{60}–C_{60}) interactions. However, in order to avoid assumptions about the nature of the solid fullerenes mixture, we have measured directly the beam composition using a mass spectrometer situated on-line with the fullerenes effusive beam (see Fig. 1). The C_{60} percentage was found to be 1–2% (a small 6:7 correction for the C_{60}:C_{70} electron impact ionization cross section was ignored). This corresponds to an enrichment factor of 5 (with respect to the 0.3% C_{60} impurity, as specified by the supplier, MER). In order to measure the final composition of the deposited fullerenes on the gold surface a TPD experiment was carried out. Again the C_{60} impurity was found to be below 2%. Fig. 9 shows the positive ion mass spectrum following Cs^+ ion impact on the C_{70}/Au target over the impact energy range of $E_0 = 100$–140 eV. There are several features that should be noted:

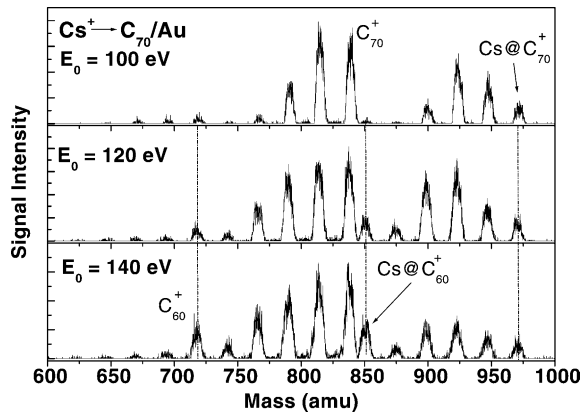

Fig. 9. Positive ion mass spectra following impact of a Cs^+ ion beam ($E_0 = 100$–140 eV) on a C_{70}/Au surface. Note the gradual formation and accumulation of the $Cs@C_{60}^+$ and C_{60}^+ ions following the fragmentation of $Cs@C_{70}^+$ and C_{70}^+.

(1) Both $Cs@C_{70}^+$ and C_{70}^+ are ejected from the surface.

(2) Using the C_2 emission sequence ($Cs@C_{70-2n}^+$ and $Cs@C_{70}^+$) as an internal thermometer for the vibrational temperature of the two parent fullerene molecules (endohedral and empty), it is clear that the $Cs@C_{70}^+$ ion is ejected from the surface much hotter than the C_{70}^+ ion. This behavior is similar to that observed for the C_{60}/Au system.

(3) At the lowest energy ($E_0 = 100$ eV) the amount of $Cs@C_{60}^+$ and C_{60}^+ generated by sequential emission of five C_2 units from $Cs@C_{70}^+$ and C_{70}^+ correspondingly is very small, below 3% of the integrated signal. However, already at 120 eV we see dramatic enhancement of the $Cs@C_{60}^+$ and C_{60}^+ ion intensities. This can be associated with the increased fragmentation of the C_{70} parent and the "stability island" behavior of the C_{60}. The very small C_{60}^+-related signal at $E_0 = 100$ eV (and below) provides further evidence to the negligible amount of C_{60} impurity within the C_{70} monolayer.

(4) The smallest endohedral daughter ion that could be identified at this stage is $Cs@C_{54}^+$.

In future experiments we will try to detect smaller fragments down to $Cs@C_{50}^+$ in order to see if we can observe the same end point (of the C_2 emission sequence), as that observed for C_{60}. It is interesting to mention that the relative intensities in the fragmentation pattern ($Cs@C_{60-2n}^+$ and $Cs@C_{70-2n}^+$) observed in our surface collision experiments corresponds to a much colder parents ($Cs@C_{60}^+$ and $Cs@C_{70}^+$) as compared with the gas phase (C_{60}:C_{70}) experiments. With K^+ collisions [12], the highest intensity fragments ($E_0 \approx 70$ eV) were $K@C_{52}^+$ and $K@C_{62}^+$, respectively, and the relative $K@C_{60}^+$ and $K@C_{70}^+$ ion intensities ($E_0 \leq 60$ eV) were very small. For Xe^+/C_{60} collisions [22] (comparable in size with Cs^+) no $Xe@C_{60}^+$ or $Xe@C_{58}^+$ were observed. The endohedral ion sequence was found to start at $Xe@C_{56}^+$. Similar behavior was observed also for Ar^+ and Kr^+ [22] projectiles. This behavior is in agreement with a weaker vibrational excitation of the parent endohedral in the surface implantation experiments due to loss of a fraction of the impact energy E_0 to surface excitations. Note that charge transfer exoergicity for the Xe^+/C_{60} case is relatively small (4.25 eV) [22] and is not expected to change this conclusion.

Finally, we would like to speculate a little bit on the transition mechanism from $Cs@C_{70}^+$ and C_{70}^+ to $Cs@C_{60}^+$ and C_{60}^+ correspondingly. The ellipsoidal C_{70} shape can be obtained from the spherical C_{60} by adding an equatorial belt of five C_2 units between two C_{30} hemispheres, thus forming a ring of five hexagons. Rotating now the two separated C_{30} hemispheres by 36° will complete the transition. The transition from C_{60} to C_{70} was suggested to involve the sequential but correlated C_2 dimers absorption in a self-promoting way [4]. Similarly, we can envision the nearly correlated loss of five C_2 units as a self-promoting mechanism where the emission of one C_2 unit facilitates the sequential emission of the next C_2 unit by partially relieving the strain caused by the first C_2 loss. This will inevitably lead to efficient accumulation of C_{60} species when the vibrational energy in the parent C_{70} species is increased, in line with the experimental observations.

4. Conclusions

The formation of endohedral fullerenes ($Cs@C_{60}^+$ and $Cs@C_{70}^+$) following the collision of low energy (35–220 eV) Cs^+ ions with C_{60} and C_{70} molecules deposited on gold and silicon surfaces was studied. Evidence is given for the single collision nature of the combined (nearly simultaneous) penetration/ejection step. Following penetration, the Cs^+ ion is trapped inside the rapidly closing cage but is left with enough backward momentum to lift the whole endo-complex off the surface. The strong deformation of the cage upon the initial impact, the annealing (bond forming) step and the back and forth scattering of the Cs^+ trapped inside the cage (chattering), are all leading to strong vibrational excitation of the outgoing endohedral. The hot $Cs@C_{60}^+$ and $Cs@C_{70}^+$ starts to emit C_2 units during their flight time to the detector, resulting in a series of $Cs@C_{60-2n}^+$ ($n = 1$–5) and $Cs@C_{70-2n}^+$ ($n = 1$–7) daughter ions. These fragmentation patterns are indicative of the initial vibrational temperature of the corresponding parent endohedrals. The sequential emission of C_2 units (shrink wrap mechanism) and the termination of the series at $Cs@C_{50}^+$ (for Cs^+ collisions with C_{60}/Au and C_{60}/Si) constitute a solid proof for the endohedral nature of the complex. Empty fullerenes (C_{60} and C_{70}) were also sputtered from the surface following the Cs^+ ion bombardment. Their fragmentation pattern suggests a weaker vibrational excitation as compared with that of the endohedral fullerenes. For both surfaces the impact energy-dependent yield of $Cs@C_{60}^+$ is peaking in the range of 75–90 eV. The ionization of the outgoing fullerenes (empty and endohedrals) probably takes place partially at the surface following charge exchange and partially on-flight via vibrationally induced electron emission. The relative contribution of each channel is not known at this stage. We believe that these experiments where the endohedral fullerenes is both being formed and scattered off the surface within the same Cs^+ collision

event constitute a unique example for a single collision pick-up scattering involving the formation of an endo-complex.

Acknowledgements

This research was supported by a grant from the Israel Science Foundation, the German–Israeli foundation (GIF), the James–Frank Program and the Technion VPR fund.

References

[1] H. Kang, M.C. Yang, K.D. Kim, K.Y. Kim, Int. J. Mass Spectrom. Ion Process. 174 (1998) 143.
[2] R. Middleton, Nucl. Instrum. Methods 144 (1977) 373.
[3] A. Kaplan, A. Bekkerman, B. Tsipinyuk, E. Kolodney, J. Chem. Phys. 117 (2002) 3484.
[4] M.S. Dresselhaus, G. Dresselhaus, P.C. Eklund, Science of Fullerenes and Carbon Nanotubes, Academic Press, San Diego, CA, 1996.
[5] H. Shinohara, Rep. Prog. Phys. 63 (2000) 843.
[6] R. Tellgmann, N. Krawez, S.H. Lin, I.V. Hertel, E.E.B. Campbell, Nature (London) 382 (1996) 407.
[7] E.E.B. Campbell, R. Tellgmann, N. Krawez, I.V. Hertel, J. Phys. Chem. Solids 58 (1997) 1763.
[8] R. Shimshi, R.J. Cross, M. Saunders, J. Am. Chem. Soc. 119 (1997) 1163.
[9] T. Weiske, D.K. Böhme, J. Hrusak, W. Kratschmer, H. Schwarz, Angew. Chem. 103 (1991) 989.
[10] T. Weiske, D.K. Böhme, J. Hrusak, W. Kratschmer, H. Schwarz, Angew. Chem. Int. Ed. Engl. 30 (1991) 884.
[11] Z. Wan, J.F. Christian, S.L. Anderson, Phys. Rev. Lett. 69 (1992) 1352.
[12] Z. Wan, J.F. Christian, Y. Basir, S.L. Anderson, J. Chem. Phys. 99 (1993) 5858.
[13] J.F. Christian, Z. Wan, S.L. Anderson, J. Chem. Phys. 99 (1993) 3468.
[14] A.V. Hamza, M. Balooch, Chem. Phys. Lett. 198 (1992) 603.
[15] E.I. Altamann, R.J. Colton, Surf. Sci. 295 (1993) 13.
[16] A.V. Hamza, M. Balooch, Chem. Phys. Lett. 201 (1993) 404.
[17] D. Klyachko, D.M. Chen, Phys Rev. Lett. 75 (1995) 3693.
[18] A. Kaplan, Y. Manor, A. Bekkerman, B. Tsipinyuk, E. Kolodney, submitted.
[19] E.E.B. Campbell, R.D. Levin, Ann. Rev. Phys. Chem. 51 (2000) 65.
[20] A. Bekkerman, B. Tsipinyuk, A. Budrevich, E. Kolodney, J. Chem. Phys. 108 (1998) 5165.
[21] F.D. Weiss, J.L. Elkind, S.C. O'Brien, R.F. Curl, R.E. Smalley, J. Am. Chem. Soc. 110 (1988) 4464.
[22] Y. Basir, S.L. Andreson, J. Chem. Phys. 107 (1997) 8370.
[23] N.W. Ashcroft, N.D. Mermin, Solid State Physics, Holt–Saunders, New York, 1976.
[24] (a) C. Pan, M.S. Chandrasekharaiah, D. Agan, R.H. Hauge, J.L. Margrave, J. Phys. Chem. 96 (1992) 6752;
(b) C. Pan, M.P. Sampson, Y. Chai, R.H. Hauge, J.L. Margrave, J. Phys. Chem. 95 (1991) 2944.
[25] M. Sai Baba, T.S. Lakshmi Narasimhan, R. Balasubramanian, N. Sivaraman, C.K. Mathews, J. Phys. Chem. 98 (1994) 1333.